Non-intuitive rotational reorientation in collisions of NO(A $^2\Sigma^+$) with Ne from direct measurement of a four-vector correlation

Thomas R. Sharples, Joseph G. Leng, Thomas F. M. Luxford, Kenneth. G. McKendrick, Pablo G. Jambrina, F. Javier Aoiz, David W. Chandler, and Matthew L. Costen

Accepted Manuscript

Published on-line in Nature Chemistry 27th August 2018

http://dx.doi.org/10.1038/s41557-018-0121-9

Non-intuitive rotational reorientation in collisions of NO(A $^2\Sigma^+$) with Ne from direct measurement of a four-vector correlation

Thomas R. Sharples[1], Joseph G. Leng[1], Thomas F. M. Luxford[1], Kenneth. G. McKendrick[1], Pablo G. Jambrina[2,3], F. Javier Aoiz[4], David W. Chandler[5]*, and Matthew L. Costen[1]*

[1]Institute of Chemical Sciences, Heriot-Watt University, Edinburgh, EH14 4AS, UK.
[2]Departamento de Química Física Aplicada, Facultad de Ciencias, Universidad Autónoma de Madrid, 28049, Madrid, Spain.
[3]Departamento de Química Física, Facultad de Ciencias Químicas, Universidad de Salamanca, 37008, Salamanca, Spain
[4]Departamento de Química Física I, Facultad de Ciencias Químicas, Universidad Complutense de Madrid, 28040 Madrid, Spain.
[5]Combustion Research Facility, Sandia National Laboratory, Livermore, CA 94550, USA.
*Correspondence to: m.l.costen@hw.ac.uk (M.L.C.), chand@sandia.gov (D.W.C.)

Abstract:

Stereodynamic descriptions of molecular collisions concern the angular correlations which exist between vector properties of the motion of the participating species, including their velocities and rotational angular momenta. Measurements of vector correlations provide a unique view of the forces acting during collisions, and a stringent test of electronic structure calculations of molecular interactions. In this work, we present the first direct measurement of the four-vector correlation between initial and final relative velocities and rotational angular momenta in a molecular collision. This property, which quantifies the extent to which a molecule retains a memory of its initial sense of rotation, or handedness, as a function of scattering angle, yields unprecedented insight into the dynamics of a molecular collision. We report surprising changes in the handedness for specific states and scattering angles, reproduced by classical and quantum scattering calculations. Comparison to calculations on different ab initio potential energy surfaces demonstrates this measurement's exquisite sensitivity to the underlying intermolecular forces.

Main Text:

The behaviour of gas phase environments such as flames, Earth's atmosphere and the interstellar medium are largely determined by collisions between their constituent molecules.[1-3] Collisions may result in chemical reaction, but the majority are non-reactive encounters. A subset of these non-reactive collisions result in transfer of energy between the various modes of motion of the partners; these *inelastic* collisions control the rates of thermalization of non-equilibrium systems, for example in the collisional deactivation of highly energetic reaction products. The experimental elucidation of inelastic collision dynamics has progressed through degrees of sophistication, from the measurement of integral cross sections for transfer between different internal energy states of the collision partners to *stereodynamics* measurements that quantify the spatial anisotropy of the encounter. The latter have been shown to be a particularly effective probe of the *ab initio* electronic structure calculations that provide the most accurate models of intermolecular interactions.

Stereodynamics measurements are typically expressed in terms of angular correlations between vector properties of the collision system. A commonly measured example is the differential cross section (DCS), which quantifies the correlation between the initial and final relative velocities of the collision partners, **k** and **k′**, respectively.[4-7] Another common measurement involves preparing a sample of molecules with a polarized angular momentum distribution, and observing the kinetics of the decay of this polarization through collisions with a bath gas, which reveals the correlation between the initial and final angular momenta of the initially-polarized collision partner, **j** and **j′**, respectively.[8-11] As well as these two-vector correlations, a number of experiments have measured three-vector correlations, such as the dependence of product angular momentum polarization on scattering angle, or **k**-**k′**-**j′** correlation.[12-16] The Stark effect has been employed to orient the bond axis of one of the collision partners prior to scattering and to explore the impact of different bond axis orientations on the DCS, a **k**-**r**-**k′** correlation.[17,18] In his 1986 Nobel Lecture, Dudley Herschbach looked forward to the prospect of measurements of the four-vector **k**-**j**-**k′**-**j′** correlation in reactive scattering, and highlighted the resolution of features of a collision otherwise lost through averaging over unresolved initial and final conditions, including the relative senses of rotation of reactants and products.[19] Subsequent theoretical work has provided formalisms in which four-vector correlation measurements may be expressed and determined from quantum scattering calculations.[20,21] There have been a few reports of experiments whose measurements contain information on this correlation, in particular the two-colour sub-Doppler circular dichroism experiments probing Li_2 + rare gas collisions by McCaffery and co-workers.[22,23] In a recent study of low-temperature HD + D_2 collisions, Perreault *et al.* interpreted structure in the angular distribution of scattered HD as a manifestation of a four-vector correlation through comparison with calculated m_j-m_j' state-to-state cross sections, exploiting the reduction in the number of partial waves at low collision energies.[24] Irregular diffraction structures in the DCS for small scattering angles in collisions of ground state NO with the rare gases have been shown by Onvlee *et al.* to be due to propensities for the largest Δm_j transitions.[25] This conclusion, a further example of an experimental observation that depends on this four-vector correlation, also relied on comparison with quantum scattering calculations. To the best of our knowledge, however, no direct, quantitative measurement of any four-vector correlation for molecular scattering has been reported in the literature.

Here we report on experiments in which optical preparation of electronically excited NO($A^2\Sigma^+$) molecules in a crossed molecular beam (CMB) apparatus[7] and detection of scattered products using velocity map imaging (VMI)[26] is used to measure a **k**-**j**-**k′**-**j′** correlation for inelastic scattering with Ne. The specific property examined is the scattering angle dependence of the orientation of **j′** arising from an initially oriented **j**: the **k**-**k′**-**j′** correlation specific to this initial **j** distribution. Figure 1 illustrates two possible scenarios occurring at different scattering angles for molecules with **j** initially pointing along the direction of approach. The upper half of the illustration shows a scattering angle for which the molecule's sense of rotation is preferentially retained during the collision, while the lower half shows a scattering angle for which the angular momentum has been substantially reoriented and is now pointing more antiparallel than parallel to the initial direction of approach. Impulsive collisions are expected to lead to the first scenario,[27,28] and a number of authors[29-31] have previously postulated that a $\Delta m_j = 0$ selection rule is generally followed in molecular collisions. As we shall discuss, however, our experiments are able to demonstrate that there is no such general propensity. The clearest demonstration of this is our observation of the second, much less intuitive, scenario of a change in the sense of rotation of the NO(A) molecule, which occurs for certain combinations of scattering angle and final state. By comparison with quantum and quasi-classical dynamics calculations, we examine the extent to which such surprising dynamical behaviour can be

captured in a classical model of the scattering. We also demonstrate the high sensitivity of this vector correlation to the interaction between the two colliders, which makes its measurement an exceptionally discriminating test of quantitative models of intermolecular forces.

Results

Figure 2 shows a schematic of the experimental setup. A molecular beam of NO molecules seeded in Ne is intersected at right angles with a beam of pure Ne. Circularly polarized light at 226 nm is used to state-selectively prepare NO($A^2\Sigma^+$; v = 0; N = 2, j = 1.5) molecules with a distribution of **j** that is *oriented*. This means that there is a preferred sense of rotation of the molecules, or, equivalently, a preference for a given sign of the m_j quantum number when defined relative to **k**.[32] The angular distribution of **j** varies as a function of time, as discussed more fully below, and makes an average angle of $\theta_j \approx \arccos\left(\langle cos(\theta_j)\rangle\right) = 65°$ with **k**. The propagation direction of the preparation laser is close to being parallel to **k** such that the angular momentum distribution before and after the collision is cylindrically symmetric about this axis. After 370 ns, the NO(A $^2\Sigma^+$; v = 0; N') products are state-selectively ionized using [1 + 1′] REMPI *via* the E $^2\Sigma^+$ state, employing circularly polarized 600 nm light, counter-propagating relative to the preparation laser beam, to effect the E←A transition in order to give sensitivity to the orientation of the products. Velocity-mapping optics accelerate the NO^+ ions onto a position-sensitive micro-channel plate/phosphor screen detector. The images resulting from these experiments are a two-dimensional projection of the velocity distribution of the scattered products onto a plane containing the initial laboratory-frame velocities of the two molecular beams.

The orientation of the scattered products is manifested in a difference in the ionization probability between experiments using right- and left- circularly polarized (RCP and LCP, respectively) probe light[33] and varies with the scattering angle, θ. We define the co- and counter-rotating probe geometries, referring to the cases in which an observer looking along **k** would see the electric fields of the preparation and probe light rotating in the same or opposite senses, respectively. We measure the normalized difference between ion signal obtained with these two probe polarizations:

$$C(\theta) = \frac{I_{co}(\theta) - I_{counter}(\theta)}{I_{co}(\theta) + I_{counter}(\theta)} \quad (1)$$

$C(\theta)$ depends on moments of the distribution of the NO(A) rotational angular momentum.[34] Throughout this paper we label moments of this distribution of the initial state $A_{q\pm}^{\{k\}}$ and the scattering-angle-dependent moments for the final state $T_{q\pm}^{\{k\}}(\theta)$. A measured value of $C(\theta)$ for a given final state depends strongly on the $T_0^{\{1\}}(\theta)$ moment, which quantifies the orientation of the NO(A) rotational angular momentum along **k**, but also has a weaker dependence on the $T_0^{\{2\}}(\theta)$ moment quantifying the alignment, or preference for a magnitude of m_j:[33]

$$C(\theta) = \frac{3h^{\{1\}}(j)T_0^{\{1\}}(\theta)}{2 - h^{\{2\}}(j)T_0^{\{2\}}(\theta)} \tag{2}$$

The $h^{\{k\}}(j)$ terms quantify the sensitivity of the probe scheme to the orientation and alignment. For an initially unpolarized distribution of **j** it is not possible to induce an orientation along **k** and $T_0^{\{1\}}(\theta) = 0$, and therefore $C(\theta) = 0$, for all θ. For such an isotropic distribution, orientation may only be induced along the axis perpendicular to both **k** and **k′**, and measurements of the resulting $T_{1-}^{\{1\}}(\theta)$ moment have previously been performed for scattering with initially unpolarized **j**.[13,14] However, by orienting **j** with respect to **k** prior to collision, the system becomes chiral and non-zero values of $C(\theta)$ can be observed in the products. Positive and negative signs of $C(\theta)$ for a given final state indicate that the final state preferentially rotates in the same and opposite sense as the initial state, respectively, while a value of zero indicates complete loss of the initially prepared orientation. The magnitude of $C(\theta)$ is therefore proportional to the initially prepared orientation, which must be known in order to interpret $C(\theta)$.

The polarization of the initial state undergoes significant oscillations over the period between preparation and probing as a result of hyperfine interactions between the initially oriented angular momentum **j** and the ^{14}N nuclear spin.[32] This polarization is measured by probing the initially-prepared state as a function of the time between the preparation and probe laser, as discussed more fully in Supplementary Information Section 1. Collisions occur stochastically between preparation and probing, and the time average of the polarization of the initial state, $C(prep) = 0.51 \pm 0.01$, may be taken as an effective pre-collision polarization to a very good approximation. In the scattering experiments, the initial sample therefore consists of NO(A) molecules with a known velocity and orientation, and, of course, this initial orientation is the same regardless of the final scattering angle.

Figure 3 shows scattering images recorded for final states $N' = 4 - 9$ in the two probe polarizations. The intensity differences between images in the two polarizations arise because of the orientation of the products. $C(\theta)$ can be determined by integrating the co- and counter-rotating image intensity in strips perpendicular to **k**. Figure 4 shows the results of this analysis for each final state.

The simplicity of an atom + diatom collision system facilitates comparison of experiments with a quantum treatment of the inelastic scattering problem, which may be used to rigorously test the potential energy surface (PES) used in the dynamics calculations to describe the intermolecular interactions. We have performed calculations of $C(\theta)$ using the Hibridon[35] time-independent quantum scattering (QS) codes and two PESs for the NO(A) + Ne system; the 2006 PES of Pajón-Suárez *et al.*,[36] henceforth referred to as the PRRH PES, and the 2012 PES of Cybulski and Fernández,[37] henceforth referred to as the CF PES. These PESs were both calculated using the RCCSD(T) method, a high-level treatment, but differ in the choice of basis set and the density of geometries at which energies were calculated. The results are plotted with the experimental measurements in Figure 4. The qualitative behaviour is very well reproduced for all quantum states by both PESs. There are, however, regions of significant quantitative disagreement with experiment, particularly for the calculations for $N' = 5 - 7$ on the CF PES, where the PRRH PES performs significantly better. Both PESs overestimate the magnitude of the negative values of $C(\theta)$ for $N' = 5$.

In addition to QS calculations, we have also performed quasi-classical trajectory (QCT) calculations of $C(\theta)$ on the same two PESs, and these are also plotted in Figure 4. The QCT calculations reproduce all of the major features observed experimentally. In particular, negative values of $C(\theta)$ for $N' = 5$ are reproduced in the classical calculations, although there are differences in the magnitude and range of scattering angles over which this occurs. We also note that the QCT calculations of $C(\theta)$ for both PESs are almost identical.

Discussion

The variation in orientation transfer behaviour exhibited by different N' states is striking. For the low N' states, the **k-j-k′-j′** correlation is very strong, in that $C(\theta)$ varies dramatically with θ. This variation becomes weaker for the high-N' final states. Perhaps the most interesting behaviour is observed for $N' = 5$, in which $C(\theta)$ becomes negative for $\theta \sim 60$–$100°$, indicating that for this range of scattering angles, the scattered molecules have lost their initial handedness and show some preference for rotation in the *opposite* sense to that in which they were rotating before the collision. This is a particularly intriguing example of the hitherto unobserved dynamics that can be made visible through measurements of this four-vector correlation.

The dependence of the post-collision NO(A) orientation on scattering angle and final state reveals the variation in propensity for transfer between the initial and final m_j states. This orientation *transfer* is distinct from previous measurements of the *collision-induced* orientation in NO(X $^2\Pi$) + Ar scattering, a three-vector **k-k′-j′** correlation, which measures the orientation induced along the perpendicular to the **k-k′** plane.[13,14] The variation in the propensities for transfer between different m_j states is substantial: the occurrence of positive and negative values of $C(\theta)$ observed over different ranges of θ in $N' = 5$ shows that in the former case there is a preference for m_j to retain the same sign, while in the latter case the propensity for m_j sign-changing collisions results in a net reversal of the handedness of the NO rotation. As in the low-collision energy study by Perreault *et al.*[24] and the analysis of low scattering angle diffraction structures by Onvlee *et al.*,[25] these variations in m_j-changing propensities make it clear that there is, in fact, no generally applicable $\Delta m_j = 0$ selection rule for molecular collisions of the kind previously postulated.[29-31]

By comparing with quantum and classical scattering calculations on two PESs for this system we are able to address two questions regarding the **k-j-k′-j′** correlation. The first is whether the additional resolution of the dynamics in this four-vector correlation measurement makes it a more sensitive probe of the PES for the collision system than the more conventional three-vector **k-k′-j′** correlation. The second is how far the dynamics revealed by this measurement, particularly the surprising change in the sense of rotation for $N' = 5$, may be described in a classical model for the scattering, and how far quantum mechanics must be invoked to understand this effect.

While QS calculations on both PESs reproduce the qualitative features of the experimentally measured values of $C(\theta)$, they differ quite substantially from one another, and the PRRH PES clearly provides a significantly better quantitative prediction of the measured dynamics. The fact that the CF PES performs less well than the PRRH PES is somewhat surprising, since the CF PES was calculated with greater angular resolution than the PRRH PES, and with a larger basis set. In previous work on the NO(A) + Ne collision system, we found close agreement for **k-k′** and **k-k′-j′** correlations between experimental measurements and QS calculations on both

of these PESs, but that neither PES perfectly reproduced experiment.[15] The level of agreement was worse at a higher collision energy, most likely a consequence of the low density of *ab initio* points in the repulsive region for both PESs. The better agreement seen here for the PRRH PES may be a result of a (coincidentally) better extrapolation into the areas of the repulsive wall probed in these new experiments. The significant differences between the calculated values of $C(\theta)$ are a consequence of the much greater sensitivity of the four-vector correlation to the PES relative to two- and three-vector correlations, since it involves less averaging over the NO(A) initial states. This is illustrated and discussed more fully in Supplementary Information Section 3. The areas of disagreement pertain to significant portions of the scattered flux; for example, the imperfectly-reproduced region of negative $C(\theta)$ for $N' = 5$ makes up approximately 25 % of the total scattering into this state. Any disagreement between experiment and theory discernible for this simple atom + diatom system has significant implications for the ability of the methods employed to make accurate predictions in more complex systems.

The QCT calculations reproduce the main features in the measured $C(\theta)$, which indicates that the observed behaviour has a classical origin. The level of agreement between the experimental results and the classical and quantum dynamics calculations becomes better for larger amounts of angular momentum transferred to the NO(A) and for larger scattering angles. Such outcomes arise preferentially from short-range, impulsive collisions in which interactions with steep regions of the repulsive wall are expected to dominate. We have also performed calculations of $C(\theta)$ for hard-shell classical scattering in which polarization is conserved along the kinematic apse, detailed in Supplementary Information Section 5. While this model does not reproduce the oscillatory or sign-changing behaviour observed experimentally for forward and sideways scattering, for strong backward-scattering close agreement is observed between experiment, kinematic apse, QCT, and QS calculations. This is strong evidence that scattering in this angular range is predominately from the rigid repulsive wall of the PES.

The observation that the QCT calculations provide a reasonably good description of the orientation transfer over the complete range of final states and scattering angles is quite a startling result, given that the effect being measured arises through preparation of an orientation in such a low-j state with a highly-quantized spatial distribution of $\mathbf{j}$. In particular, the occurrence of negative values at approximately the correct range of θ indicates that the fundamentals of this non-intuitive behaviour can be understood in terms of classical physics. There have been previous measurements of the $\mathbf{j}$-$\mathbf{j}'$ two-vector correlation that have demonstrated reversal of the orientation of a collision for parity-changing collisions of *open-shell* $^2\Pi$ molecules,[8,38] but in these cases the effect is fundamentally a quantum mechanical one since rotational parity is not a classical concept. The change in orientation that we have observed for a particular final state in NO(A) + Ne has a different origin: there is a clear correlation between the magnitude of the torque applied to the molecules and its direction, and significant variation of this correlation with scattering angle. A small proportion of the trajectories in the QCT calculations result in a change in the direction of $\mathbf{j}$ with respect to $\mathbf{k}$ and over a narrow range of scattering angles for $N' = 5$ these trajectories form a sufficiently large proportion of the scattering to lead to an overall change in sign of $C(\theta)$. Visualization of two examples of this kind of trajectory are given in the Supplementary Videos 1 and 2: on close approach to the Ne atom, the NO(A) rotation is first slowed and then accelerated on the departure of the atom, but in the opposite direction. Despite the success of the QCT calculations in rationalizing the experimental measurements, the quantum mechanical nature of the scattering should not be ignored in a complete description of the orientation transfer. A purely quantum mechanical mechanism has been shown to contribute to the collision-induced orientation in diatom-atom scattering, through comparison of QCT and QS calculations on a

hard-shell PES treating the diatomic electronic structure as closed shell,[39] and it may be possible to isolate purely quantum mechanical effects that account for the more negative values of $C(\theta)$ observed in the experiments relative to the QCT predictions. Interestingly, while the QS predictions of $C(\theta)$ are very sensitive to the PES, the QCT predictions on the two PESs are almost identical, indicating the importance of quantum mechanical effects to the particular sensitivity of this measurement to the topography of the PES.

This four-vector correlation measurement is a more stringent test of high-level electronic structure calculations than previous two or three-vector measurements. It reveals surprising, new, and non-intuitive scattering dynamics, which are only visible through this direct imaging of the relative m_j-m_j' cross sections with scattering angle resolution. The key to the measurement of the **k-j-k′-j′** correlation is the use of polarized laser radiation to prepare a molecular beam of molecules with an anisotropic angular momentum distribution. As such, this method could be applied to elucidate the dynamics of a wide range of collision systems, both inelastic and reactive. In addition to electronically excited states of other molecules, the collisions of molecules in their electronic ground states may be investigated using, for example, IR or Raman pumping schemes to prepare vibrationally excited states with polarized angular momentum distributions.[24,40,41] Such experiments will be important in the continuing drive to provide ever-more-stringent tests of the accuracy of electronic structure calculations and our understanding of intermolecular interactions.

Methods

Crossed molecular beam velocity map imaging experiments: The crossed molecular beam apparatus used to perform the experiments has been described in detail previously.[7] The NO (99.5 %, BOC) beam was a 10 % mix in Ne (100.000 %, BOC) at 3 bar backing pressure. The resulting velocity distribution was Gaussian with mean 855 m s^{-1} and full width at half maximum (FWHM) of 57 m s^{-1}. The pure Ne (100.000 %, BOC) beam had a backing pressure of 5 bar, with a Gaussian velocity distribution with a mean of 787 m s^{-1} and a FWHM of 52 m s^{-1}. These speed distributions resulted in a Gaussian distribution of centre-of-mass collision energies with a mean of 678 cm^{-1} and a FWHM of 60 cm^{-1}.

NO(A $^2\Sigma^+$, v = 0, N = 2, j = 1.5) was generated at the crossing point of the two molecular beams by excitation from NO($X^2\Pi_{½}$, v = 0, j = 0.5) *via* the R_{21}(0.5) transition of the A-X(0,0) band. The excitation light was provided by the frequency-doubled output of a Nd:YAG-pumped dye laser (Sirah CTSG/ Continuum Surelite II-10). The probe scheme only resolves nuclear rotation states N', as the transitions from individual $j' = N' \pm ½$ states are separated by frequencies that are much smaller than the Doppler width or the laser bandwidth. The excitation light was circularly polarized by a Babinet-Soleil compensator, set to generate left circularly polarized (LCP) output. The preparation laser was unfocussed, with a fluence of 0.65 mJ cm^{-2} and a beam diameter of 2 mm.

Following a 370 ns delay to allow NO(A) + Ne collisions to occur, the products were probed through 1 + 1' REMPI *via* the R(N') branch of the E-A(0,0) band. The output of a Nd:YAG-pumped dye laser (Sirah CSTG-DA24/Continuum Surelite I-10) at ~600 nm was used in the excitation to the E state, and a portion of the 532 nm output of the Nd:YAG laser was separated out and used for ionization. The probe beam had a fluence of 0.65 μJ cm^{-2}, while the fluence of the ionization beams was varied in the range 4-40 mJ cm^{-2}. Both the probe and ionization lasers had beam diameters of 3 mm. Because of the short time between preparation and probing, all scattered NO(A) molecules remain in the probe region prior to ionization and so no density-flux transform is required in the analysis of the resulting images. The polarization of the 600

nm probe light was controlled using a photo-elastic modulator (PEM) (PEM-90, Hinds Instruments).

The NO^+ ions were velocity mapped onto a microchannel plate (MCP) detector coupled to a phosphor screen (Photonis, 40 mm active diameter, P47 phosphor) with the light emitted from the phosphor recorded using a camera (Basler scA780-54fm, 782 × 582 pixel array). The voltage applied to the MCP plates was pulsed, with a 120 ns gate width, to reject ions generated by the 226 nm preparation laser.

Scattering images were acquired for both LCP and right circularly polarized (RCP) probe polarizations. For each polarization, background images in which the Ne beam was delayed by 1 ms, and therefore effectively absent, were also acquired in an interleaved sequence, in order to allow subtraction of background signals arising from non-resonant ionization of NO(A) by the ionization laser. The probe beam was scanned over the Doppler width of the probe transition to ensure unbiased detection of all scattered velocities. The laser was scanned in fifteen steps of 5×10^{-4} nm and each scan was repeated four times during a single measurement with a total of 48,000 shots across both probe laser polarizations including background signal. Between six and nine independent measurements were made for each final N' state across multiple days.

Theoretical calculations: Close-coupled quantum scattering calculations were performed using the Hibridon suite of codes. HIBRIDON is a package of programs for the time-independent quantum treatment of inelastic collisions and photodissociation.[35] The two sets of calculations employed the PRRH[36] and CF[37] PESs, which were calculated using the spin-restricted coupled cluster method with single, double and perturbative triple excitations (RCCSD(T)). An NO(A) rotational basis of channels up to N = 20 was included in the calculations, with NO(A) treated as a rigid rotor with rotational constants B = 1.987 cm^{-1} and γ = –0.0027 cm^{-1}. Calculations were performed for partial waves with $J_{tot} \leq 350.5$ and propagation from 3.5 to 300 Bohr. The output from these calculations were m_j-m_j' cross sections over 1° ranges of θ and these were used to calculate values of C(θ) as described in Supplementary Information Section 2.

The details of the QCT method for inelastic atom-rigid rotor collisions have been described previously[42] and hence we will just summarize here the most relevant computational details. Batches of 20×10^6 trajectories were run on both the CF PES and the PRRH PES for N=2, at a fixed collision energy of 678 cm^{-1}. An integration step of 2×10^{-16} s was used, that guarantees a total energy conservation better than one part in 10^5, and the Ne-NO(A) starting and final distance were chosen to be 10 Å. Since QCT calculations on both PESs were performed assuming the NO molecule as a rigid rotor at its equilibrium distance, the method of Lagrange multipliers was used, to keep the NO distance fixed throughout the trajectory. To assign the final state for each trajectory, the square of the rotational angular momentum, N', was first calculated, and their values were rounded to the nearest integer.

The $T_0^{\{k\}}(\theta)$ scattering angle dependent moments (**k-k′-j′** polarization dependent differential cross sections) were calculated using a procedure described previously,[43] with the trajectories weighted according to the initial (extrinsic) distribution of θ_N, the angle between **N** and **k**[44,45]

$$w_i = \frac{1}{4\pi}\sum_{k=0}^{3}(2k+1)\,\langle A_0^{\{k\}}\rangle\,\langle jj,k0|jj\rangle P_k\left(\cos\theta_N^{(i)}\right) \tag{3}$$

where w_i is the weight of the i-th trajectory, $\langle..|..\rangle$ is the Clebsch-Gordan Coefficient,[44,46] P_k is the k-th order Legendre Polynomial, and $\theta_N^{(i)}$ is the value of θ_N for the i-th trajectory. The

coefficients of the expansion, $\langle A_0^{\{k\}} \rangle$ are the time-averaged moments of the initial state rotational angular momentum distribution given in Supplementary Table 1.[43] The basic equations[47,48] are given in Supplementary Information Section 4.

Data availability. The raw data on which this publication is based can be accessed via the Heriot-Watt University Data Repository.

References and Notes:

1. Wayne, R. P. *Chemistry of Atmospheres*, 3rd edn. Oxford University Press: Oxford, 2000.

2. Roueff, E. & Lique, F. Molecular Excitation in the Interstellar Medium: Recent Advances in Collisional, Radiative, and Chemical Processes. *Chem Rev* **113**, 8906-8938 (2013).

3. Najm, H. N., Paul, P. H., Mueller, C. J. & Wyckoff, P. S. On the adequacy of certain experimental observables as measurements of flame burning rate. *Combust Flame* **113**, 312-332 (1998).

4. Bishwakarma, C. K. *et al.* State-to-State Inelastic Scattering of O_2 with Helium. *J Phys Chem A* **120**, 868-874 (2016).

5. Brouard, M. *et al.* The fully quantum state-resolved inelastic scattering of NO(X) plus Ne: experiment and theory. *Mol Phys* **111**, 1759-1771 (2013).

6. de Jongh, T. *et al.* Imaging diffraction oscillations for inelastic collisions of NO radicals with He and D_2. *J Chem Phys* **147**, 013918 (2017).

7. Sharples, T. R., Luxford, T. F. M., Townsend, D., McKendrick, K. G., Costen, M. L. Rotationally inelastic scattering of NO(A $^2\Sigma^+$) + Ar: Differential cross sections and rotational angular momentum polarization. *J Chem Phys* **143**, 204301 (2015).

8. McGurk, S. J., Halpern, J. B., McKendrick, K. G. & Costen, M. L. Parity-Dependent Rotational Energy Transfer in CN(A $^2\Pi$, ν =4, j $F_1\varepsilon$) + N_2, O_2, and CO_2 Collisions. *J Phys Chem A* **118**, 2007-2017 (2014).

9. Paterson, G., Costen, M. L. & McKendrick, K. G. Collisional depolarisation of rotational angular momentum: influence of the potential energy surface on the collision dynamics? *Int Rev Phys Chem* **31**, 69-109 (2012).

10. Paterson, G., Costen, M. L. & McKendrick, K. G. Collisional depolarization of rotational angular momentum: what are the observables and how can they be measured? *Mol Phys* **109**, 2565-2585 (2011).

11. Chadwick, H. *et al.* The collisional depolarization of OH(A $^2\Sigma^+$) and NO(A $^2\Sigma^+$) with Kr. *J Chem Phys* **140**, 054306 (2014).

12. Brouard, M., *et al.* Rotational alignment effects in NO(X) plus Ar inelastic collisions: An experimental study. *J Chem Phys* **138**, 014310 (2013).

13. Brouard, M. *et al.* Rotational Orientation Effects in NO(X) plus Ar Inelastic Collisions. *J Phys Chem A* **119**, 12404-12416 (2015).

14. Lorenz, K. *et al.* Direct measurement of the preferred sense of NO rotation after collision with argon. *Science* **293**, 2063-2066 (2001).

15. Luxford, T. F. M., Sharples, T. R., McKendrick, K. G. & Costen, M. L. Experimental testing of ab initio potential energy surfaces: Stereodynamics of NO(A $^2\Sigma^+$) + Ne inelastic scattering at multiple collision energies. *J Chem Phys* **145**, 174304 (2016).

16. Luxford, T. F. M., Sharples, T. R., Townsend, D., McKendrick, K. G. & Costen, M. L. Comparative stereodynamics in molecule-atom and molecule-molecule rotational energy transfer: NO(A $^2\Sigma^+$) + He and D_2. *J Chem Phys* **145**, 084312 (2016).

17. Nichols, B. *et al.* Steric effects and quantum interference in the inelastic scattering of NO(X) plus Ar. *Chem Sci* **6**, 2202-2210 (2015).

18. Brouard, M. *et al.* Stereodynamics in NO(X) plus Ar inelastic collisions. *J Chem Phys* **144**, 224301 (2016).

19. Dudley R. Herschbach - Nobel Lecture: Molecular Dynamics of Elementary Chemical Reactions". Nobelprize.org. Nobel Media AB 2014. Web. 6 Dec 2017. <http://www.nobelprize.org/nobel_prizes/chemistry/laureates/1986/herschbach-lecture.html>.

20. Balint-Kurti, G. G. & Vasyutinskii, O. S., Vector Correlation Analysis for Inelastic and Reactive Collisions between Partners Possessing Spin and Orbital Angular Momentum. *J Phys Chem A* **113**, 14281-14290 (2009).

21. de Miranda, M. P. & Clary, D. C. Quantum dynamical stereochemistry of atom-diatom reactions. *J Chem Phys* **106**, 4509-4521 (1997).

22. Collins, T. L. D., McCaffery, A. J. & Wynn, M. J. 2-Color Sub-Doppler Circular-Dichroism - a 4-Vector Correlation Molecular-Dynamics Experiment. *Phys Rev Lett* **66**, 137-140 (1991).

23. Collins, T. L. D., McCaffery, A. J. & Wynn, M. J. 2-Color Sub-Doppler Circular-Dichroism - a 4-Vector Correlation Molecular-Dynamics Experiment for Inelastic and Reactive Collisions. *Faraday Discuss* **91**, 91-96 (1991).

24. Perreault, W. E., Mukherjee, N. & Zare, R. N. Quantum control of molecular collisions at 1 kelvin. *Science* **358**, 356-359 (2017).

25. Onvlee, J. *et al.* Imaging quantum stereodynamics through Fraunhofer scattering of NO radicals with rare-gas atoms. *Nat Chem* **9**, 226-233 (2017).

26. Eppink, A. T. J. B. & Parker, D. H. Velocity map imaging of ions and electrons using electrostatic lenses: Application in photoelectron and photofragment ion imaging of molecular oxygen. *Rev Sci Instrum* **68**, 3477-3484 (1997).

27. Khare, V., Kouri, D. J. & Hoffman, D. K. On Jz-Preserving Propensities in Molecular-Collisions. 1. Quantal Coupled States and Classical Impulsive Approximations. *J Chem Phys* **74**, 2275-2286 (1981).

28. Khare V., Kouri D. J. & Hoffman D. K. On a Jz-Preserving Propensity in Molecular-Collisions. 2. Close-Coupling Study of State-to-State Differential Cross-Sections. *J Chem Phys* **76**, 4493-4501 (1982).

29. Chandler, D. W. & Farrow, R. L. Measurement of Rotational Energy-Transfer Rates for HD (v = 1) in Collisions with Thermal HD. *J Chem Phys* **85**, 810-816 (1986).

30. McCaffery, A. J., Proctor, M. J. & Whitaker, B. J. Rotational Energy-Transfer - Polarization and Scaling. *Annu Rev Phys Chem* **37**, 223-244 (1986).

31. Sitz, G. O. & Farrow, R. L. Preparation and Decay of Alignment in N_2 (v = 1). *J Chem Phys* **101**, 4682-4687 (1994).

32. Zare, R. N. *Angular Momentum: Understanding Spatial Aspects in Chemistry and Physics*. Wiley: New York, 1988.

33. Fano, U. & Macek, J. H. Impact Excitation and Polarization of Emitted Light. *Rev Mod Phys* **45**, 553-573 (1973).

34. Orr-Ewing, A. J. & Zare, R. N. Orientation and Alignment of Reaction-Products. *Annu Rev Phys Chem* **45**, 315-366 (1994).

35. Alexander, M. H., Manolopoulos, D. E., Werner, H-J. & Follmeg, B. HIBRIDON; available at http://www2.chem.umd.edu/groups/alexander/hibridon/hib43/hibhelp.html

36. Pajon-Suarez, P., Rojas-Lorenzo, G., Rubayo-Soneira, J. & Hernandez-Lamoneda, R. The intermolecular potential of NO(A $^2\Sigma^+$)-Ne: An ab initio study. *Chem Phys Lett* **421**, 389-394 (2006).

37. Cybulski, H. & Fernandez, B. Ab Initio Ground- and Excited-State Intermolecular Potential Energy Surfaces for the NO-Ne and NO-Ar van der Waals Complexes. *J Phys Chem A* **116**, 7319-7328 (2012).

38. Norman, J. B. & Field, R. W. Collision-Induced Angular-Momentum Reorientation and Rotational Energy-Transfer in CaF(A $^2\Pi_{1/2}$)-Ar Thermal Collisions. *J Chem Phys* **92**, 76-89 (1990).

39. Brouard, M., Hornung, B. & Aoiz, F. J. Origin of Collision-Induced Molecular Orientation. *Phys Rev Lett* **111**, 183202 (2013).

40. Dong, W. R., Mukherjee, N. & Zare, R. N. Optical preparation of H_2 rovibrational levels with almost complete population transfer. *J Chem Phys* **139**, 074204 (2013).

41. Mukherjee, N., Dong, W. R. & Zare, R. N. Coherent superposition of M-states in a single rovibrational level of H_2 by Stark-induced adiabatic Raman passage. *J Chem Phys* **140**, 074201 (2014).

42. Aoiz, F. J., Verdasco, J. E., Herrero, V. J., Rabanos, V. S. & Alexander, M. A. Attractive and repulsive interactions in the inelastic scattering of NO by Ar: A comparison between classical trajectory and close-coupling quantum mechanical results. *J Chem Phys* **119**, 5860-5866 (2003).

43. de Miranda, M. P., Aoiz, F. J., Banares, L. & Rabanos, V. S. A unified quantal and classical description of the stereodynamics of elementary chemical reactions: State-resolved k-k'-j' vector correlation for the H+D_2(v=0, j=0) reaction. *J Chem Phys* **111**, 5368-5383 (1999).

44. de Miranda, M. P. & Aoiz, F. J. Interpretation of quantum and classical angular momentum polarization moments. *Phys Rev Lett* **93**, 083201 (2004).

45. Brouard, M. & Vallance, C. (ed.). *Tutorials in Molecular Reaction Dynamics*. Royal Society of Chemistry: Cambridge, 2010.

46. Aldegunde, J. *et al.* How reactants polarization can be used to change and unravel chemical reactivity. *J Phys Chem A* **109**, 6200-6217 (2005).

47. Aoiz, F. J., Brouard, M., Eyles, C. J., Klos, J. & de Miranda M. P. The collisional depolarization of $^{(2S+1)}\Sigma$ radicals by closed shell atoms: Theory and application to OH(A $^2\Sigma^+$)+Ar. *J Chem Phys* **130**, 044305 (2009).

48. Brouard, M., Chadwick, H., Eyles, C. J., Aoiz & F. J., Klos, J. The k-j-j ' vector correlation in inelastic and reactive scattering. *J Chem Phys* **135**, 084305 (2011).

Acknowledgments

This work was supported by the U.K. EPSRC *via* grants EP/J017973/01 and EP/P001459/1. J.G.L. thanks the EPSRC for the provision of a DTP studentship (EP/N509474/1). T.F.M.L.

acknowledges Heriot-Watt University for a James Watt PhD scholarship. P.G.J. and F.J.A. acknowledge funding by the Spanish Ministry of Science and Innovation (grant MINECO/FEDER-CTQ2015-65033-P) and E. Verdasco for support with the calculations. P.G.J. acknowledges funding by Fundación Salamanca City of Culture and Knowledge. The work of D.W.C. was supported by the US Department of Energy, Office of Basic Energy Sciences, Division of Chemical Sciences, Geosciences, and Biosciences, under Grant 2019 SNL 17014098. Sandia National Laboratories is a multi-mission laboratory managed and operated by National Technology and Engineering Solutions of Sandia, LLC., a wholly owned subsidiary of Honeywell International, Inc., for the U.S. Department of Energy's National Nuclear Security Administration under contract DE-NA-0003525. We also acknowledge the assistance of P. J. Dagdigian, J. Kłos and M. H. Alexander in performing the quantum scattering calculations. Raw data on which this publication is based can be accessed via the Heriot-Watt University Data Repository.

Author Contributions

The research project was conceived and supervised by M.L.C. The experiments were carried out by T.R.S., J.G.L., T.F.M.L., and D.W.C. Data analysis was performed by T.R.S. and J.G.L. Quantum scattering calculations were carried out by T.R.S. Quasi-classical trajectory calculations were performed by P.G.J. and F.J.A. Kinematic apse calculations were performed by M.L.C. and T.R.S. The results were interpreted by T.R.S., P.G.J., F.J.A., D.W.C, K.G.M. and M.L.C. The paper was written by T.R.S. with contributions from all authors.

Additional Information

Supplementary information is available in the online version of the paper. Correspondence and requests for materials should be addressed to M.L.C.

Competing Financial Interests

The authors declare no competing financial interests.

Figure Captions

Figure 1: Illustration of two possible correlations between the initial and final rotational angular momentum, resolved at different scattering angles. In the upper trajectory, there is a preference for the angular momentum to point along its initial direction, while in the lower trajectory the direction of the angular momentum has been changed and the molecules preferentially rotate in the opposite sense.

Figure 2: Schematic of the experimental setup and Newton diagram showing the directions of the velocity vectors describing the colliders before collision. The velocities of the NO and Ne colliders are labelled $\mathbf{v}_{NO}$ and $\mathbf{v}_{Ne}$, respectively. Also shown is the initial relative velocity $\mathbf{k}$ and centre-of-mass velocity $\mathbf{v}_{CoM}$. This is superimposed on an example scattering velocity map image. The preparation and probe lasers counter-propagate and are parallel to $\mathbf{k}$.

Figure 3: **Velocity map images used to measure the k-j-k′-j′ correlation**. Co- and counter-rotating images for each N' final state averaged over all experimental measurements. The colour-intensity maps applied to the two images for each state are comparable with one another, and are brightest at the maximum scattered ion intensity for each state, but intensities cannot be compared between states. The image intensity is different for probing in the two geometries because of the orientation of the rotational angular momentum of the scattered molecules relative to **k**, which can only be observed because they were prepared with an orientation relative to this axis prior to collision. This intensity difference varies both with final state and scattering angle, indicating a four-vector **k-j-k′-j′** correlation that depends on the final state.

Figure 4: **Measured and calculated values of $C(\theta)$ for each N' final state, revealing the variation of the orientation transfer with scattering angle.** Mean experimentally measured values (black squares) with error bars indicating twice the standard error of the mean. QS calculations on the CF PES (red line) and PRRH PES (blue line) PES. QCT calculations on the CF PES (green line) and PRRH PES (magenta line). Negative values of $C(\theta)$ indicate that the products are oriented in the opposite sense with respect to **k** relative to their initial orientation. While the experimentally measured values are better reproduced by the QS calculations, the major features are also reproduced by the QCT calculations, indicating that the orientation transfer can be understood classically. The QS calculations on the two PESs are significantly different from one another, demonstrating the sensitivity of the measurement to small differences in the PES.

Figure 1

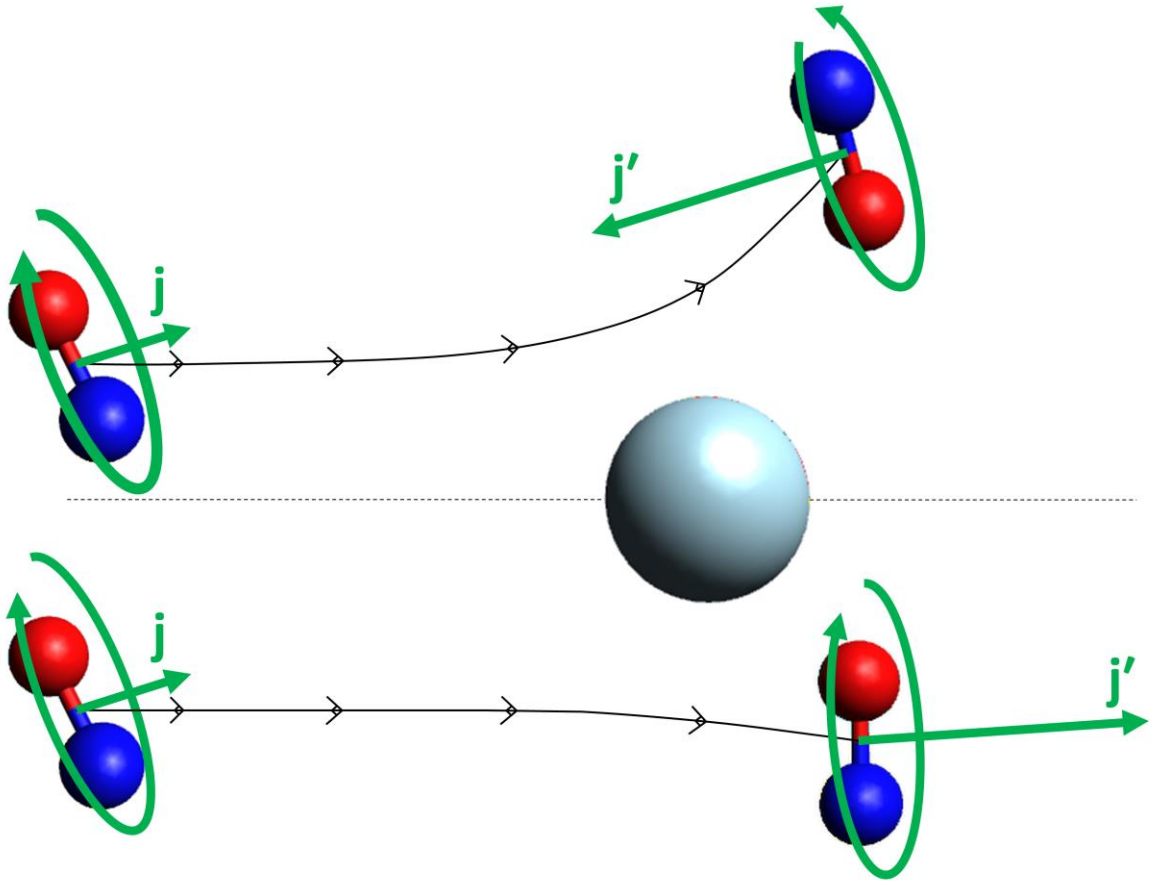

Figure 2

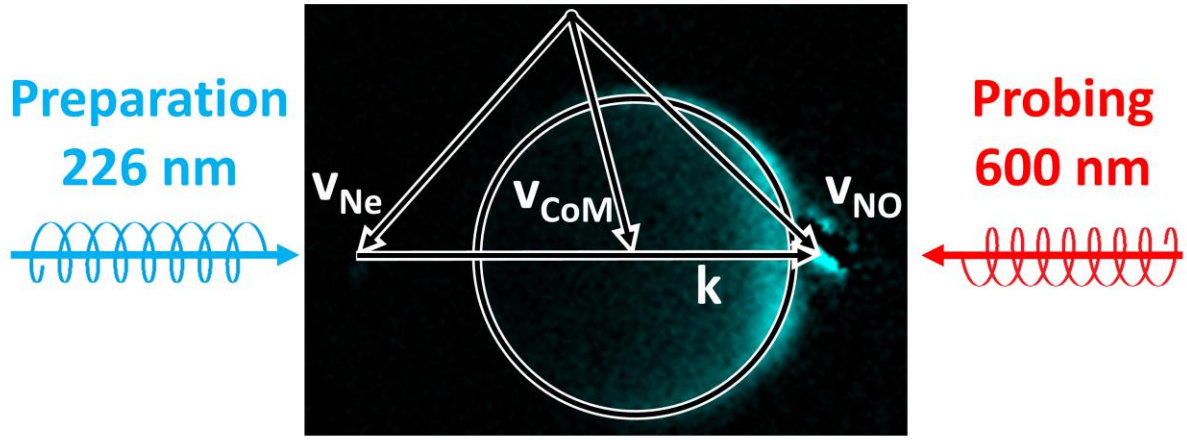

Figure 3

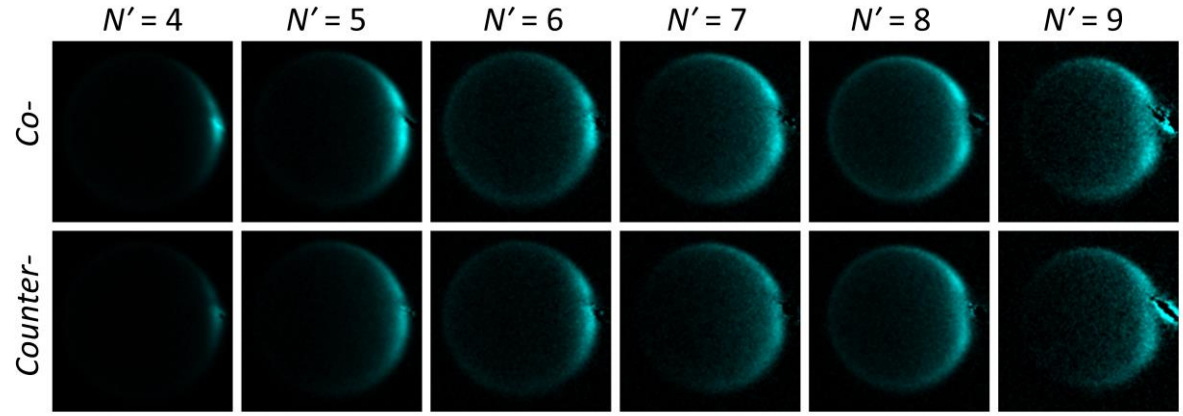

Figure 4